

Growth Kinetics of Gold Nanoparticles

L.E. Murillo*, O.Viera*, E.Vicuña*, J.G. Briano*, M.Castro*, Y. Ishikawa**, R. Irizarry***, L. Solá***

*University of Puerto Rico, Mayagüez Campus, Mayagüez, Puerto Rico, j_briano@rumac.uprm.edu

**University of Puerto Rico, Río Piedras Campus, San Juan, Puerto Rico

*** DuPont Microelectronics, Manatí, Puerto Rico

ABSTRACT

We have measured the growth kinetics of gold nanoparticles in real time. Gold nanoparticles were formed from the reduction of gold (III) in aqueous solution and monitored with a stopped-flow reactor equipped with a diode array. The overall reduction of gold (III) occurred in less than 20 [ms]. The growth kinetics was determined from measurements of the plasmon resonance time-dependent wavelength. The peak position and width of the plasmon resonance were found to be sensitive to particle size and to the medium dielectric constant. The maximum peak wavelength shifts toward higher wavelengths with particle size. The results were modeled with Mie's scattering theory. Excellent agreement between theory and experiment were found in the peak maximum and long wavelength tail, for particle sizes less than 50 [nm]. The dependence of the gold dielectric constant on particle size and the effect of multi-pole interactions must be added if a theoretical path is to be followed.

Keywords: Gold nanoparticles, growth, kinetics, plasmon, Mie.

INTRODUCTION

Supersaturation is the driving force to the formation of particles in solution (crystallization or precipitation). In the case of metallic particles in aqueous media, where a reduction process is carried out, the saturation concentration of the ground atomic metal is very close to zero. In this case, atoms will nucleate to form small clusters (particles), which will grow trying to achieve a minimum in Gibbs energy. The nucleation stage is chaotic and affected by the chemical nature of the solution components, including: ionic strength, concentration level of metal, presence of surfactants, temperature, mixing, among others. After particles achieve a critical size, the growth stage take control and the importance of the nucleation regime vanishes. Seshadri et al. [1] studied the growing of colloidal gold in solution by using electron microscopy and absorption spectroscopy. Wilcoxon et al. [2] studied the aggregation kinetics of colloidal gold by measuring the polarized relaxation time. Both studies are in a much larger time frame than the present one.

To experimentally follow the formation and growth of metallic particles, the specific optical properties of small metallic particles must be used. In particular, the gold plasmon resonance may be followed in the range of 10 to ~100 [nm]. Mie's theory [3] gives a good qualitative representation of the cross section spectrum of metallic gold particles.

In this study of the formation of gold nanoparticles from solution, the reduction/nucleation/growth process takes less than 1 [s] and requires a particularly fast technique to follow the optical changes. A stopped flow reactor SFR, commonly used to study kinetics of fast reactions in solution, was used. The equipment allows almost an instantaneous perfect mixing, eliminating the mass transfer resistance to the reaction process.

MIE THEORY

The theory was developed for a single spherical particle, assuming the dielectric constant to be independent of the particle size [4]. The extinction coefficient C_{ext} is related to the Mie scattering coefficients a_n and b_n through

$$C_{ext} = \frac{2\pi R^2}{\omega} \sum_{n=1}^{\infty} n(n+1) \frac{2n+1}{n} \left(|a_n|^2 + |b_n|^2 \right) \quad (1)$$

where $x = 2\pi R n_0 / \omega$, n_0 is the refractive index of the host medium, ω is the wavelength of the incident light *in vacuo*. a_n and b_n are the scattering coefficients, which are function of the particle radius R and the wavelength in terms of Ricatti-Bessel functions. For particles with diameters less than 100 [nm], usually only the first three terms in equation (1) are needed.

Mie theory is usually presented including only dipole interactions (good for particles up to ~50 [nm]) as a relation between the cross-section of the absorption spectrum $\tilde{\sigma}$ and the incident light-wavelength $\tilde{\omega}$,

$$\tilde{\sigma} = \frac{4\pi V}{\omega} \text{Im} \left(\frac{\epsilon_m \epsilon_1}{\epsilon_m + \epsilon_2} \right) \quad (2)$$

where ϵ_m is the solvent dielectric constant, V is the particle volume, and ϵ_1 and ϵ_2 are the real and imaginary

components of the dielectric constant of the particles, ϵ_{IB} , defined as:

$$\epsilon_{IB} = \epsilon_{IB}^{\infty} - \frac{f_{IB}}{\omega^2 + \omega_{IB}^2} \quad (3)$$

The dielectric constant has an electronic component due to plasmon excitation modeled through Drude's equation, and one associated with interband transitions. In the particular case of gold particles, both components are important. The contributions of interband transition (IB) and Drude (D) to the particle dielectric constant may be expressed as:

$$\epsilon_{IB} = \epsilon_{IB}^{\infty} - \frac{f_{IB}}{\omega^2 + \omega_{IB}^2} \quad (4)$$

$$\epsilon_D = \epsilon_{\infty} - \frac{f_D}{\omega^2 + i\omega\tau} \quad (5)$$

Drude's model has been modified [5,6,7], to include particle size effects into the electronic component of the dielectric constant, according to:

$$\epsilon_{IB} = \epsilon_{IB}^{\infty} - \frac{f_{IB}}{\omega^2 + \omega_{IB}^2 + \frac{2\gamma_{IB}}{R}} \quad (6)$$

$$\epsilon_D = \epsilon_{\infty} - \frac{f_D}{\omega^2 + i\omega\tau + \frac{2\gamma_D}{R}} \quad (7)$$

where, ω_p is the frequency of the plasma oscillation of bulk gold (8.89 eV), ω_0 stands for the frequency of inelastic collisions (electron-phonon coupling, defects, impurities) of free electrons within the metal and is simply the reciprocal of the electron relaxation time τ . τ_b is the corresponding relaxation time for the bulk metal, and v_F is the electron velocity at the Fermi surface.

The interband contribution is calculated as that of the bulk metal, by subtracting the electronic contribution from the experimental dielectric constant of the metal [8].

EQUIPMENT

For this rapid process we used a stopped-flow reaction analyzer (SFR), from Applied Photophysics Ltd., London, UK. This apparatus allows the study of fast chemical and biochemical reactions in liquid media. A photo diode linear array, with 256 elements, allowing a separation of 2.17 [nm], was used to obtain the complete spectra as a function of time. The equipment has less than 2 [ms] of dead time, and allows us to take ~800 spectra in a 1 [s] period.

RESULTS

To follow the gold particle growing kinetics, we acquired several gold colloids [9,10]. Figure 1, shows the normalized absorption spectra for colloids with different particle size. The spectra were normalized to the absorption measured at the peak maximum. The wavelength that corresponds to the maximum absorption peak represents the particle plasmon excitation energy. Differences in the position of the peak as well as the width of the plasmon band are characteristic of the particle sizes [11]. Diameters less than 2 [nm] do not show a defined plasmon band due to quantum size effects. From sizes (diameter) of 5 [nm] to ~50 [nm] the system could be well described by Mie model.

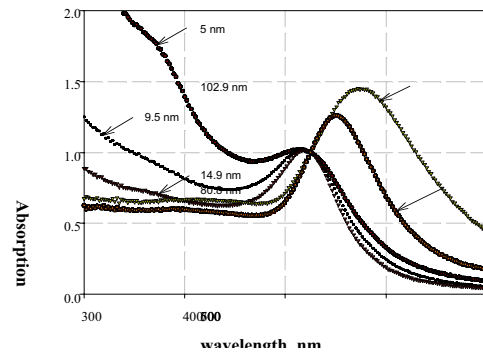


Figure 1: Absorption spectra for gold colloids of different sizes.

Relative Absorption

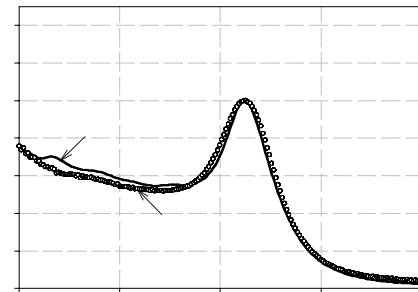


Figure 2: Absorption spectrum for a gold colloid with particles 30.9 [nm] diameter. The circles are the experimental measurements and the solid line was obtained with equation (2).

Figure 2, shows the absorption spectrum for a 30.9 [nm] gold colloid. In this case the agreement between Mie theory and experiments is excellent. However, for larger particles the model deviates strongly from the

experimental data. Thus, we use the experimental spectra of 11 gold colloids of known sizes, to establish an empirical correlation between the maximum peak wavelength and particle size.

The calibration curve relating particle size to the maximum peak wavelength is shown in Figure 3. Calculations using Mie model with quadrupole effects are shown for comparison. The dependence of the maximum peak wavelength on particle size may be described by the following exponential equation:

$$\lambda_{max} = 500 + 0.0015 \cdot e^{0.0015 \cdot d} \quad (9)$$

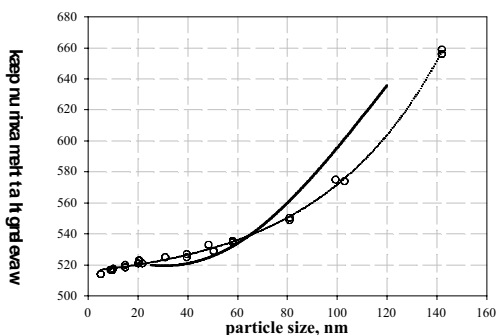


Figure 3: Wavelength at the maximum peak vs. particle size. The open circles are the experimental points, the dashed line is an exponential fit, and the solid line was obtained, with equation (1).

In Figure 4 we show the time dependent spectra for the reduction and growth of nano-size gold particles. The initial reduction stage may be followed by the depletion of the 300 [nm] band (characteristic of gold III). For the conditions of the system in Figure 4, complete reduction of gold III was attained after 15 [ms]. The nucleation stage follows reduction and cannot be analyzed clearly by just following the absorption spectrum. Plasmon resonance due to “metallic behavior” is associated to the peak in the 500 [nm] region. After 0.2–0.3 [s] the change of the plasmon band with time is clear. Displacement of the base line due to scattering effects is also observed.

Figure 5, shows the time dependence of the particle size under conditions specified on Figure 4. Particle sizes were determined with equation (9). A great disorder is observed at the beginning (time less than 0.4 [s]), due to the limitation of the theory for treating non-metallic particles, and a pattern of regular growing is notorious after 0.4 to 0.5 [s].

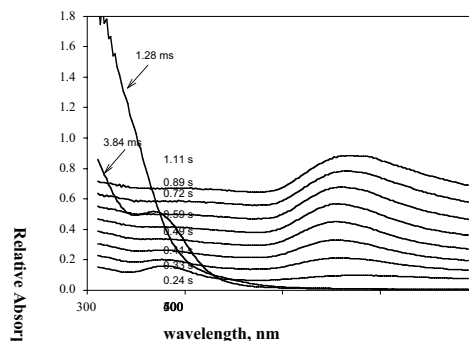


Figure 4: Gold particle growth in aqueous solution; initial concentrations: Au^{+3} [67 mM], SO_3^{-2} [185 mM]. $T = 25^\circ\text{C}$

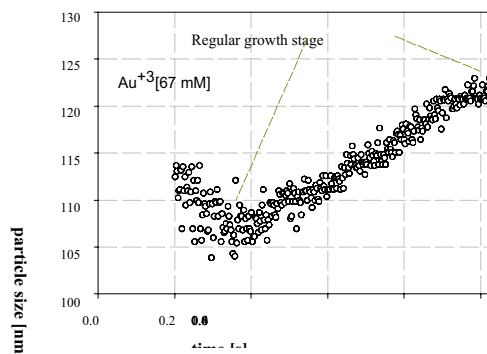


Figure 5: Growth kinetics of gold particles, Au^{+3} [67 mM], $T = 25^\circ\text{C}$

An almost linear regime is achieved after ~ 0.4 [s], suggesting a growth rate (dV/dt) proportional to the surface area of the particles. We carried out the experiment at a much lower initial concentration of gold, maintaining about the same initial proportion of the reducing species over the gold III concentration. This case is plotted in Figure 6, for a period of 2 [s]. The initial stage is similar to the previous case, but the particle size where the linear regime begins is smaller. For times longer than 1.5 [s], the scattering of the data increases notoriously. This is due to aggregation and sedimentation, in addition to the possible deposition of gold at the walls of the absorption cell.

In Figure 7, we show a fitted linear regression for the growth of gold nanoparticles, as a function of time, for three levels of initial gold concentration, in the range of 0.4 to 1 [s]. Within the region, the slopes for the three cases are almost identical and not affected by the metal initial concentration. Increasing the initial concentration of Au^{+3} results in the formation of larger particles at the initial stages of the growth process.

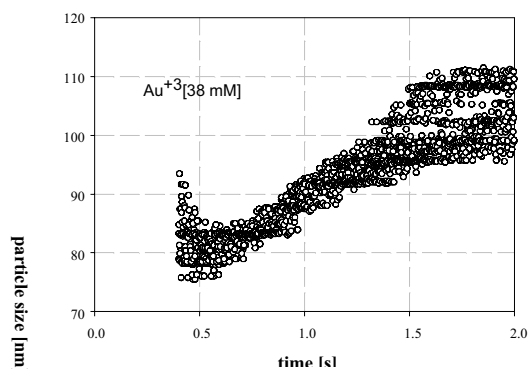


Figure 6: Growth kinetics of gold particles, Au^{+3} [38 mM], $T = 25^\circ\text{C}$

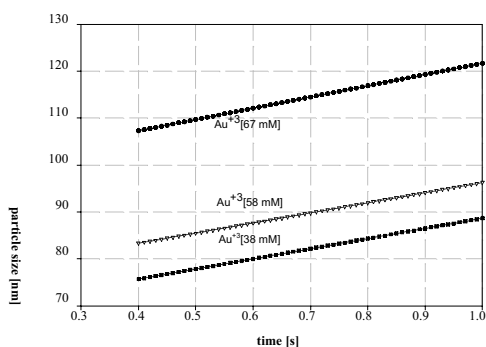


Figure 7: Linearized growth kinetics.

CONCLUSIONS

The growth kinetics of gold nanoparticles may be experimentally followed by collecting the absorption spectra in real time. The particle surface area controls a stage in the growth process.

The wavelength of the maximum absorption peak is directly related to particle size. Mie equation may be used to quantitatively represent the optical properties of gold particles if the change of the dielectric constant with particle size is appropriately incorporated into the model. For particles with diameters larger than 50 [nm], quadrupole interactions must be considered.

REFERENCES

- [1] R. Seshadri, G.N. Subbana, V. Vijaykrishnan, G.U. Kulkarni, G. Ananthakrishna and C.N.R. Rao, *J.Phys. Chem.* 99, 5639, 1995.
- [2] J.P. Wilcoxon, J.E. Martin and D.W. Schaefer, *Phys. Rev. A* 39, 2675, 1989.
- [3] G. Mie, *Ann. Phys.*, 25,377, 1908.

[4] U. Kreibbig, G. Bour, A. Hilger and M. Gartz, *Phys. Stat. Sol. (a)* 175, 351, 1999

[5] U. Kreibbig and C.Z. v. Fragstein, *Z. Phys.*, 224, 307, 1969.

[6] M.M. Alvarez, J.T. Khoury, T. Gregory Schaaff, M.N. Shafigullin, I. Vezmar and R. L. Whetten, *J. Phys. Chem. B*, 101, 3706, 1997.

[7] V. I. Roldughin, *Russ. Chem. Rev.*, 69, 821, 2000.

[8] P.B. Johnson and R.W. Christy, *Physical Review B*, 6, 4370, 1972.

[9] M. Hayat (Ed.) "Colloidal Gold. Principles, Methods, and Applications," Academic Press, New York, 1989.

[10] G. Schmid (Ed.) "Clusters and Colloids. From Theory to Applications," Weinheim: VCH, New York, 1994.

[11] S. Link and M.A. El-Sayed, *J. Phys. Chem. B*, 103, 4212, 1999.